IPP-Report

IPP Max-Planck-Institut für Plasmaphysik

M. Hoek, H.-S. Bosch, W. Ullrich

Triton Burnup Measurements at ASDEX Upgrade by Neutron Foil Activation

IPP 1/320
March 1999

Triton Burnup Measurements at ASDEX Upgrade by Neutron Foil Activation

M. Hoek*, H-S Bosch and W. Ullrich
Max-Planck-Institut für Plasmaphysik
8046 Garching bei München
Germany

Abstract

A system for neutron activation of foils for the measurement of triton burnup in ASDEX Upgrade plasmas has been installed. The calibration factors, relating the global neutron flux to the local flux at the position of the foils, were calculated by MCNP. The input file for MCNP was written with emphasis on the internal structure of the vacuum vessel. Especially regions close to the irradiation point were carefully modeled. It was found that the calibration parameters were not dependent on the structure far away from the irradiation point, e.g. the lower divertor. An important conclusion from this is that with the installation of the new "Divertor II" in ASDEX Upgrade, the calibration parameters are not expected to change.

The yield of the 2.45 MeV neutrons is measured by activation of indium foils. The results from these measurements are cross-calibrated with the time-integrated yield from an U-238 fission chamber. It was found that the yield from activation is systematically 17±12 % higher than the yield obtained from the fission chamber.

The 14.1 MeV neutrons were measured by activation of copper and silicon foils. The burnup was then determined by the fractional yield $Y_{14.1}/Y_{2.45}$. The measured values of the burnup are in the range of 0.1-1.9 %, depending on the plasma parameters.

Classically, the triton burnup is expected to increase with the electron temperature as $\sim T_e^{1.5}$. In ASDEX Upgrade, this is also the case for relatively large values of the effective charge number, Z_{eff}. However, for smaller Z_{eff} it is found that the triton burnup increases as $\sim T_e^{2.0\text{-}2.2}$.

The measurements of triton burnup are compared with simulated values of the burnup utilizing the code CONFINE. It was found that systematically the measured values are smaller than the simulated ones but the difference becomes smaller as the triton burnup increases.

---

* Present address:
University of Tokyo, Dept. of Quantum Engineering and Systems Science
7-3-1 Hongo, Bunkyo-ku
Tokyo 113-8656, Japan

1. Introduction

Studies of fast charged particles produced in magnetically confined deuterium (DD) plasmas are of fundamental interest since the results from such studies may anticipate the behavior of future deuterium-tritium (DT) reactor plasmas. An example of such a fast particle is the 1 MeV triton from the D(D,p)T reaction which has a similar gyroradius as the 3.5 MeV alpha particles from D(T,n)α. These alpha particles will provide the necessary energy for a self-sustained burning plasma in a future DT reactor, but slow down 3 times faster than the MeV tritons. This means that the fast triton is more sensible to non-classical effects and therefore the motivation for measurements of these tritons is further increased. In this work we have studied the emission of 2.5 MeV neutrons from the D(D,n)^{3}He reaction which indicate the birth of a 1 MeV triton population and the emission of 14 MeV neutrons from D(T,n)α which provides information regarding the confinement, slowing down and losses of these tritons.

In a deuterium plasma, 1 MeV tritons are produced by D(D,p)T in approximately the same rate as 2.5 MeV neutrons from D(D,n)^{3}He. The tritons are then slowed down, mainly due to Coulomb interactions with electrons but also with ions as the triton energy gets reduced. The DT fusion cross section for a cold deuterium target with the tritons as projectile particles, is maximized at an energy of ~170 keV (lab frame). During slowing down, the tritons are subject to prompt losses, i.e. losses of full energy tritons whose orbits intersect the wall because of large drifts, banana orbit losses and ripple losses, which rise from inhomogenities in the magnetic field along the triton path. A fraction of the confined tritons is "burned up" by the reaction D(T,n)^{4}He. The generated 14.1 MeV neutrons can be measured and the fraction 14.1 MeV/2.5 MeV neutrons then gives a direct number of the triton burnup.

The cross sections of the relevant reactions for the process of triton burnup versus the energy (CM frame) are shown in fig. 1. The parametrizations of the cross sections have been described in ref. [1].

The most important parameters for the amount of tritons that undergo burnup is the current density profile, J(r), whose strength determines the degree of confinement, and the electron temperature profile, $T_e(r)$, which essentially controls the slowing down of the tritons. The probability for burnup in its turn is directly proportional to the time of the slowing down.

The energy loss, dE/dT, of the triton is normally described by the classical energy loss formula [2] which omits the contribution from the electric field parallel to the triton velocity:

$$\left\langle \frac{dE}{dt} \right\rangle = -\frac{\alpha}{\sqrt{E}} - \beta E \qquad (1)$$

The coefficients α and β describe slowing down on ions ("ion-drag") and on electrons ("electron-drag") respectively, and can be written as:

$$\alpha = 1.81 \cdot 10^{-13} \ln \Lambda_{ii} \sqrt{A} Z^2 \sum_j \frac{n_j Z_j^2}{A_j}$$
$$\beta = 3.18 \cdot 10^{-15} \ln \Lambda_{ie} \frac{Z^2}{A} \frac{n_e}{T_e^{3/2}} \quad (2)$$

A and Z are the mass- and atom numbers of the tritons and n is the density [m^{-3}] and T_e is the electron temperature [eV] of the plasma. Index j denotes the species of the bulk plasma. In the calculations of the critical energy and slowing down time in this paper, a pure deuterium plasma

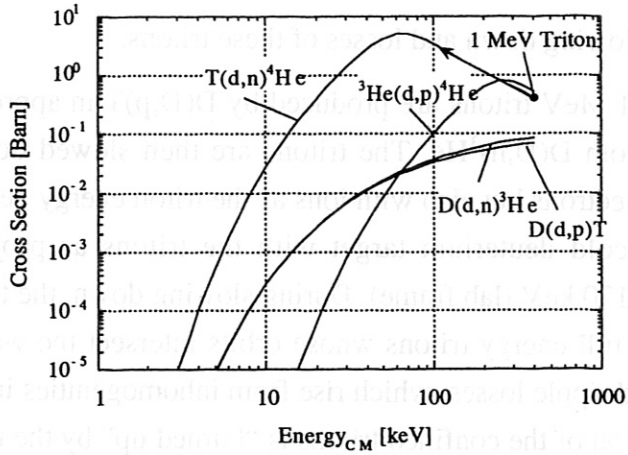

Figure 1. *Cross sections of the relevant reactions for triton burnup versus the energy in the center-of-mass (CM) system. 2.5 MeV neutrons are generated from the D(D,n) reaction at approximately the same rate as 1 MeV tritons (E_{CM} = 400 keV) which are generated from the D(D,p) reaction. The 1 MeV tritons slow down in the plasma and a fraction gets "burned up" by the D(T,n) reaction. The generated 14.1 MeV neutrons can then be measured to derive the triton burnup.*

with the deuterium density equal to the electron density has been assumed. The coefficients Λ_{ie} and Λ_{ii} are the Coulomb logarithms for ion-electron and ion-ion collisions respectively, and can be expressed as:

$$\ln \Lambda_{ie} = 32.1 - \ln\left(\frac{\sqrt{n_e}}{T_e}\right)$$
$$\ln \Lambda_{ii} = \ln \Lambda_{ie} + 9.03 - \frac{\ln T_e}{2} \quad (3)$$

From Eq. (1) it is clear that for high triton energies, it is the electron drag which is the dominant process for the slowing down of the tritons. The energy at which the ion drag equals the electron drag is called the critical energy, E_{crit}, and can be calculated by setting the ion drag term equal to the electron drag term in Eq. (1):

$$E_{crit} = \left(\frac{\alpha}{\beta}\right)^{2/3} \tag{4}$$

High electron temperatures of the plasma raise the critical energy and increases the importance of ion-drag. The critical energy for the tritons in typical ASDEX Upgrade plasmas is 80-90 keV.

The time of the triton slowing down from the initial energy E_0 to the plasma ion temperature, T_i, can be derived from Eq. (1):

$$\tau_s = \int_{E_0}^{kT_i} \left\langle \frac{dE}{dt} \right\rangle^{-1} = \frac{2}{3}\frac{1}{\beta} \ln\left(\frac{1+(E_0/E_{crit})^{3/2}}{1+(kT_i/E_{crit})^{3/2}}\right) \approx \frac{2}{3}\frac{1}{\beta} \ln\left(1+\left(\frac{E_0}{E_{crit}}\right)^{3/2}\right) \tag{5}$$

The last equality is valid if the kinetic energy of the ions, kT_i is small compared to the critical energy and this is normally the case.

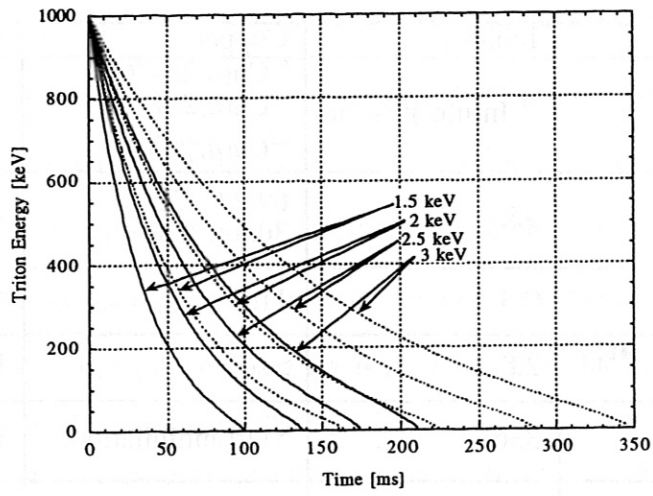

Figure 2. *Time evolution of the triton energy for electron densities of 10^{16} (dashed lines) and 10^{20} m^{-3} (solid lines), and different electron temperatures of the target plasma.*

The calculated evolution of the triton energy for electron densities of 10^{16} and 10^{20} m^{-3} is shown in fig. 2. A typical slowing down time of the tritons in ASDEX Upgrade plasmas is ~200 ms.

2. Measurement Technique

For the measurements of the 2.5 MeV and the 14.1 MeV neutrons we have employed neutron activation of high-purity foils. The use of high-purity foils is motivated by the necessity to avoid competing activity, mainly from (n, γ) reactions. For this diagnostic, a pneumatic rabbit transfer system of polyethylene capsules containing the foils was designed and installed. The transfer time from the measurement station with the HP-Ge gamma detector to the irradiation position was about 20 s and the foils were irradiated just behind the upper divertor, less than ~15 cm from the plasma edge and 1 m from the center of the plasma.

Table 1 *Neutron induced reactions used for the neutron activation measurements at ASDEX Upgrade. The table shows the reaction, the isotopic abundance of the interesting nuclei, the neutron threshold energy and the neutron energy at which the reaction cross section is maximum. The competing neutron reactions with copper are shown in italics. Also shown is the emitted γ-energy from the daughter nucleus, the γ-abundance and the half-life of the daughter nucleus. The diameter and thickness of the foils were 2 cm and 1 mm respectively. The weights of the foils were typically: 2.2 g (In), 2.6 g (Cu) and 0.7 g (Si).*

Mtrl:	Indium	Copper	Silicon
Reaction:	^{115}In(n,n')^{115}mIn	^{63}Cu(n,2n)^{62}Cu *^{65}Cu(n,2n)^{64}Cu* *^{63}Cu(n,γ)^{64}Cu*	^{28}Si(n,p)^{28}Al
Isotopic abund.: [%]	95.7	69.2 (^{63}Cu) 30.8 (^{65}Cu)	92.2
Thresh. energy: [MeV]	0.3	11.5	4
Max cross section at: [MeV]:	2.8	>16	10.4
γ-energy: [keV]:	336	511 (annihilation)	1779
γ-abundance: [%]	45.9	195	100
Half-life:	4.5 h	9.7 min	2.2 min

The main advantage with activation technique is that the irradiated materials can be positioned inside the vessel, very close to the plasma without any regards of electric or radiation background problems. There might be some concerns for magnetic materials, e.g. iron, however, in our case, we only used indium-, copper- and silicon foils, which are not susceptible for magnetic fields. The measurements of the decaying daughter nucleus may be done in a location far away from the neutron source. The measurement equipment is simple and reliable consisting of a HP-Ge γ-detector, a linear amplifier and an ADC. The drawbacks are that the measurement

procedure is not easily automated and that the obtained neutron yields are time integrated. Furthermore, high total neutron yields are necessary (>10^{14} neutrons/shot for ASDEX Upgrade) and the errors become large mainly due to the difficulty to obtain an accurate calibration which relates the local and the global neutron yield.

For the measurements, we have routinely irradiated 3 foils simultaneously. Indium was used for the measurements of the 2.45 MeV neutrons and copper and silicon for the measurement of the 14.1 MeV neutrons. We also tried aluminum foils for high performance shots but were unable to get any useful data.

After an irradiation time of ~5 s, the foils were transferred back to the gamma measurement station where, with exception for the silicon foils, they were stored for a certain amount of time before the gamma measurement. Typical "cooling times" for the foils were 3-4 h for the indium foils and 1-2 h for the second measurement of the copper foils. The silicon- and the first measurement of the copper foils were measured immediately.

The time integrated value of the neutron yield can be calculated according to (see ref. [3]):

$$S_n = \frac{C \cdot M}{\alpha_\gamma \varepsilon(E_\gamma) e^{-\lambda t_1}(1-e^{-\lambda \Delta t}) \alpha_{Is} m N_A \int \Phi(E)\sigma(E)dE} \qquad (6)$$

where C is the measured number of γ-counts from the daughter nuclide during a measurement time Δt, M is the molar mass of the nuclide, α_γ is the γ -abundance (fraction of the measured γ-line per disintegration) and $\varepsilon(E_\gamma)$ is the efficiency of the γ-detector for the γ-energy E_γ. Furthermore, λ is the decay constant of the daughter nuclide, t_1 is the cooling time of the irradiated sample, α_{Is} is the isotopic fraction of the nuclide, m is the mass of the sample and N_A is Avogadros constant. The integral $\int \Phi(E)\sigma(E)dE$ is the calibration factor relating the local yield to the total yield from the plasma source. The error analysis and the equation for calculating the neutron yield from copper measurements have been described in ref. [4].

2.1 Neutron activation

For the measurements of the 2.5 MeV neutrons, we have employed neutron activation of indium foils. Activation of indium is an excellent choice due to the threshold energy of 300 keV (thermal neutrons are filtered), the maximum cross section at 2.8 MeV, and the simple γ-measurement.

The measurements of the 14 MeV neutrons were done by neutron activation of materials with threshold energies above 2.5 MeV, i.e. silicon and copper, where copper is the most sensitive of these materials. The analysis of the irradiated silicon foils is the most straightforward

of these two, with only one measurement. The analysis of the irradiated copper foils is complicated by competing neutron reactions, which implies at least two measurements of the γ-decay of the daughter nucleus. The daughter nuclide of the $^{63}Cu(n,2n)$ reaction decays by β^+. Furthermore, the competing reactions $^{63}Cu(n,\gamma)$ (β^+, E_{thr}: thermal) and $^{65}Cu(n,2n)$ (β^+, E_{thr}: 10.5 MeV) must be corrected for. Also, for β^+-decays there is always the case of escaped β^+ from the foil which means that the measured annihilation photons are too low. The procedure for the analysis of the foils has been described in refs. [3, 4]. The main characteristics for the different foils are shown in table 1.

During the measurement period 1996, ~200 measurements, with 3 foils per measurement, were done. Not counting disrupted shots, shots with Ne-puff and shots with too low yield of neutrons; ~130 In-measurements, ~120 Cu-measurements and only ~10 Si-measurements remained.

2.2 Monte Carlo calculations of the calibration factors

From the γ-measurements of the activated foils we can calculate the number of neutrons that has reacted with the foil (if the neutron cross sections are known). However, to get the relation between this number and the total emitted number of neutrons from the plasma, we need to calculate or measure a calibration factor. This calibration factor depends mainly on the energy- and the spatial distribution of the neutrons emitted from the plasma and the tokamak geometry with its material composition surrounding both the neutron source and the irradiation position. These factors then determine the energy distribution of the neutron flux at the irradiation position. From this distribution together with the cross sections for the relevant neutron reactions in the foil, one can calculate a calibration factor. The simplest would be to introduce a well calibrated neutron source or a neutron generator [5] inside the tokamak vacuum vessel to get a relation between the number of source neutrons and the decay gamma's from the irradiated foils. However, available neutron sources like ^{252}Cf are generally too weak for a calibration of the neutron activation system and we did not have access to any neutron generator. The remaining alternative is to calculate the neutron energy distribution per emitted source neutron by means of Monte Carlo. However, such simulations imply large errors due to the difficulty in modeling the complex 3-dimensional geometry of the machine itself, the modeling of the neutron source distribution (the plasma) and the inaccuracy of the used cross sections (~5-10 %). The uncertainty in these calculations gives the dominant uncertainty in the measurements of the neutron yield from neutron activation technique. Furthermore, the accuracy is difficult to estimate because the different sources of errors are difficult to quantify.

The energy distribution of the neutron flux/source neutron has been calculated using the MCNP code [6]. The input file for MCNP was based on the work described in ref. [7]. For

symmetry reasons, only one octant needed to be modeled. The two vertical planes, which separate the octant from the rest of the geometry, are reflecting surfaces for the neutrons. The original purpose of this model was to estimate the radiation levels of the tokamak surroundings due to neutron activation. Therefore, the modeling of the internal structure in the vessel and the neutron source were less detailed. In our case we are mainly interested in the neutron flux inside the torus which made it necessary to add e.g. upper and lower divertors, a graphite limiter and a proper source distribution.

In the modeling, the ASDEX Upgrade components have been described by ~190 surfaces which are combined into the specification of ~150 cells. Components around the irradiation point such as the capsule and the pneumatic transfer tube have been carefully modeled. Furthermore it was necessary to model a fusion plasma source for inclusion in the source code of MCNP. The plasma source distribution is described by a probability distribution of the neutron source density, s(r), according to (see refs. [8, 9]):

$$s(r) = \left[1 - \left(\frac{r}{a}\right)^2\right]^4, \quad 0 \le r \le a \tag{7}$$

where the parameter a is the minor plasma radius and r/a is the normalized plasma radius.

The parameter r determines a constant flux surface and corresponds to a magnetic flux line which can be represented by:

$$R = R_0 + r\cos(t + \delta \sin t) + e\left[1 - \left(\frac{r}{a}\right)^2\right], \tag{8}$$

$$z = Er\sin t$$

where

$$\delta = \delta_0 \frac{r}{a}, \quad 0 \le r \le a, \quad 0 \le t \le 2\pi \tag{9}$$

R is the radial distance to the torus axis and z is the poloidal distance to the torus midplane. For ASDEX Upgrade we used the following parameters for the simulation of a "typical" plasma:

R_0 = 165 cm;	major plasma radius
a = 50 cm;	vertical minor plasma radius
E = 80/50 = 1.6;	elongation (horizontal plasma radius / vertical plasma radius)
e = 10 cm;	eccentricity (estimation of the Shafranov shift)
δ_0 = 0.1;	maximum triangularity of the plasma.

With the above description of the source, we have assumed that the nuclear fusion reactions emit neutrons isotropically. However, especially for NBI heating with deuterium beams, this assumption is not true. In this work we have assumed that the corrections for the anisotropic emission of the neutrons are negligible.

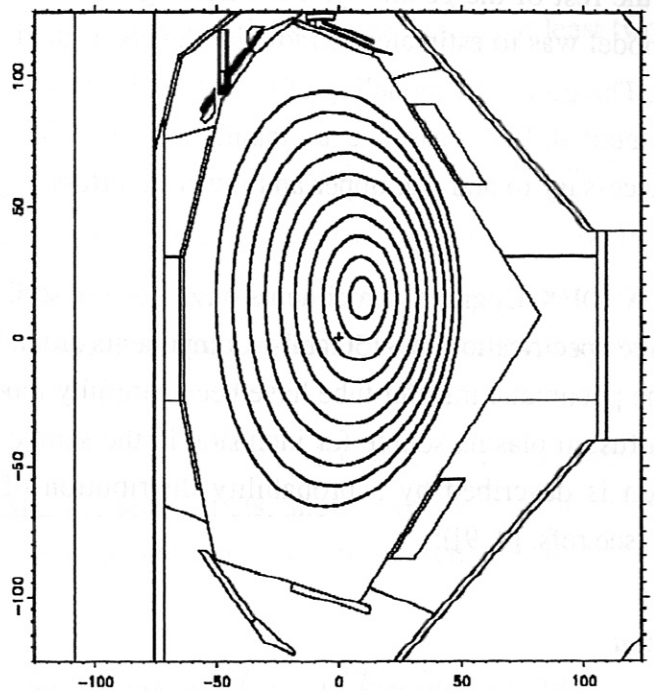

Figure 3. *Poloidal cross section of the tokamak geometry as modelled for MCNP. The x- and y-axis are in dimensions of [cm]. The model includes the end part of the irradiation pneumatic tube for the neutron activation at (x=~-50, y=~100), the upper divertor, the inner graphite limiter and the divertor at the bottom of the vessel. Also shown is the modelled fusion plasma source where the inner constant flux surface corresponds to* $r/a = 0.1$ *while the outer constant flux surface corresponds to* $r/a = 1.0$.

Fig. 3 shows a part of the modeled geometry for the MCNP. The figure (except for the source distribution) is generated by the plot routines of MCNP and is a poloidal cross section of the geometry. The upper divertor, the inner graphite limiter, the divertor in the bottom, the toroidal passive stabilizers (PSL) and the front end of the pneumatic transfer tube are clearly visible. The modeled plasma source is overlaid over the figure where the inner flux surface corresponds to r/a = 0.1 while the outer surface corresponds to r/a = 1.0. The geometrical descriptions also include the vacuum vessel with the ports, the poloidal and toroidal coils, the center column assembly, the floor and the walls surrounding the whole tokamak experiment hall.

As a calibration factor we have calculated the reaction rate per nucleus and source neutron. The reaction rate, R, within the sample can be written as:

$$R \propto \int_{E_{cutoff}}^{E_0} \Phi(E)\sigma(E)dE \qquad (10)$$

where $\Phi(E)$ is the neutron flux (per source neutron) at the irradiation point calculated by Monte Carlo and $\sigma(E)$ is the cross section for the neutron reaction. E_0 is 2.45 MeV for the calibration of the indium foil measurements and 14.1 MeV for the copper- and silicon foil measurements. E_{cutoff} was chosen to 0.2 MeV and is the cutoff neutron energy for the Monte Carlo calculations.

Table 2 shows the calculated calibration factors ("Flux integrals") for 2.45 and 14.1 MeV

Table 2. *Calculated calibration factors ("Flux integrals") for 2.45 MeV neutrons (In-foil) and for 14.1 MeV neutrons (In-, Cu- Si- and Al-foil). Calculations with different types of geometries, another set of cross sections, and a line source was done as a sensitivity check.*

Modeling	**Flux integral (In) [10^{-24}]**	**Flux integral (Cu) [10^{-24}]**	**Flux integral (Si) [10^{-24}]**	**Flux integral (Al) [10^{-24}]**
Full modeling with plasma source	$7.7 \cdot 10^{-7}$ (±6.3%)	$6.5 \cdot 10^{-7}$ (±8.9%)	$5.1 \cdot 10^{-7}$ (±8.0%)	$1.4 \cdot 10^{-7}$ (±7.7%)
Voided lower divertor and lower stabilizer (PSL)	$7.7 \cdot 10^{-7}$ (±6.0%)	-	-	-
Voided divertors and PSL	$9.9 \cdot 10^{-7}$ (±4.7%)	-	-	-
Other set of cross sections	$8.2 \cdot 10^{-7}$ (±5.1%)	-	-	-
Line source	$8.8 \cdot 10^{-7}$ (±6.3%)	-	-	-

source neutron energies and for four different foils, In-, Cu, Si- and Al-foils. Initially it was planned that we could utilize the $^{27}Al(n,p)^{27}Mg$ reaction but the neutron yields were too low for that measurement. We also investigated how sensitive the modeling was for the calculation of the calibration factor for In by removing ("void") parts of the geometry from the modeling. It was found that if the lower divertor and the lower stabilizer were removed, which are components far away from the irradiation position, the calibration factor increased by 0.5 %, which is within the uncertainty of the original calibration factor (6.3 %). However, if the upper stabilizer and the upper divertor also were voided, the calibration factor increased by 28%. This is a clear indication for the importance of a careful modeling around the irradiation point.

For a check of the importance of the modeled plasma source we calculated the calibration factor using a line source. The calibration factor then increased by 14 %. The reason for this is that the fraction direct/scattered neutrons that hit the irradiation point is larger and that the cross section for direct, full-energy, neutrons are larger than for scattered neutrons.

For Maxwellian plasmas, the source neutron energy distribution is Gaussian with a FWHM described by ([10]):

$$\Delta E_{FWHM} = k\sqrt{T_i}\ [keV] \tag{11}$$

where T_i is the ion temperature [keV] and k is weakly ion temperature dependent. k is often approximated by 82.5 for D(D,n)^{3}He reactions.

At TFTR different source neutron energy distributions were simulated for the MCNP calculations of the calibration factors [11]. It was found that the energy distribution was important only for materials whose threshold energies were above 13 MeV. The change of the calibration factors for the dosimetric reactions with threshold energies less than 12 MeV was merely a few percent. Therefore, we used monoenergetic neutrons for all our MCNP calculations.

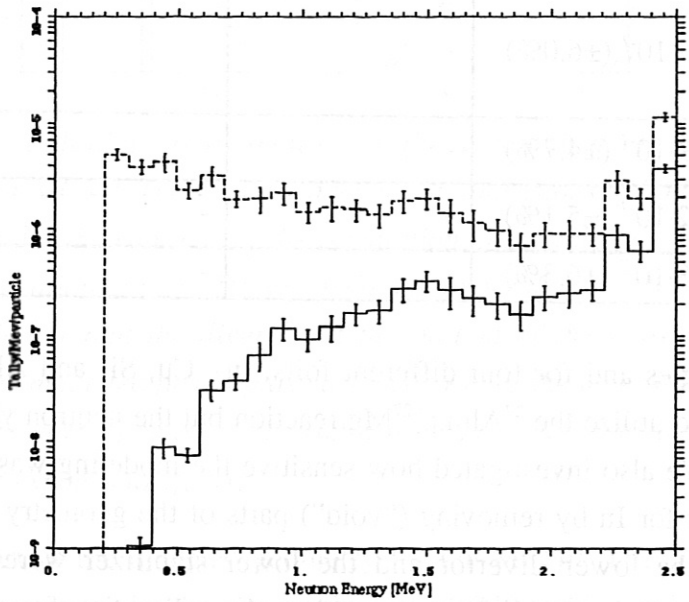

Figure 4. *Neutron flux energy distribution at the irradiation position for a neutron source energy of 2.45 MeV (staggered line). Also shown is the number of reactions/MeV per source neutron that occur with ^{115}In. An integration of this distribution gives the calibration factor in unit of [10^{-24}].*

Fig. 4 shows the calculated flux at the irradiation position for a neutron source energy of 2.45 MeV. Also shown is the number of reactions/MeV per source neutron with indium, in units of [10^{-24}]. Due to the threshold energy of 300 keV, the thermal neutrons do not influence the results, making the Monte Carlo calculation more reliable. Fig. 5 shows the corresponding plot for 14.1 MeV neutrons and the number of reactions/MeV per source neutron for a copper foil.

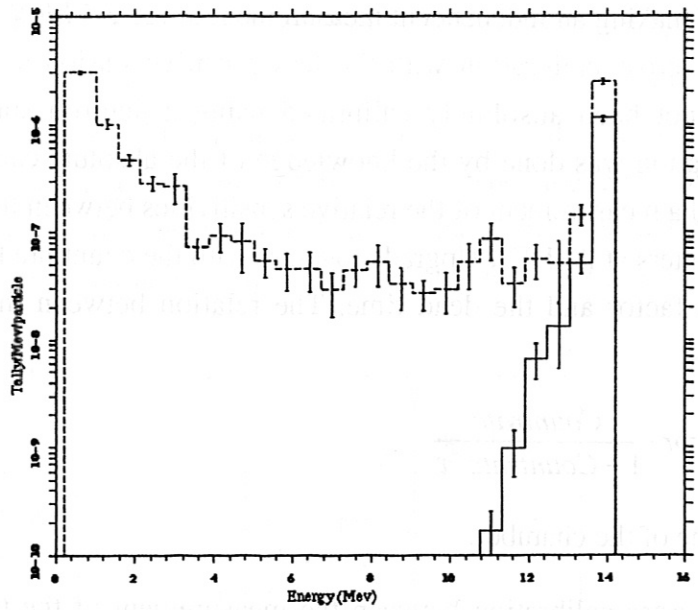

Figure 5. *Neutron flux energy distribution at the irradiation position for a neutron source energy of 14.1 MeV (staggered line). Also shown is the number of reactions/MeV per source neutron that occur with ^{63}Cu. An integration of this distribution gives the calibration factor in unit of [10^{-24}].*

3. Measurements and Results

3.1 Fission chamber cross calibration

Measurements of the 2.5 MeV neutrons, utilizing In-foils, were routinely done for the measurements of the triton burnup. In principle, we could have used the time-integrated yield obtained from the U-238 chamber instead. However, the reason for using the activation method

Table 3. *Neutron counters at ASDEX Upgrade. The relation between the neutron rate and the count rate is given by Eq. (12).*

Detector	Count rate [kHz]	Cal. factor	Dead time [s]
U-238	3-700	$3.27 \cdot 10^{10}$	$5.0 \cdot 10^{-7}$
U-235B	10-1100	$9.25 \cdot 10^{7}$	$3.1 \cdot 10^{-7}$
U-235A	4-1200	$3.39 \cdot 10^{7}$	$2.8 \cdot 10^{-7}$
BF-3	10-80	$1.35 \cdot 10^{6}$	$4.1 \cdot 10^{-6}$
He-3	10-180	$3.82 \cdot 10^{5}$	$1.8 \cdot 10^{-6}$

for both 2.5 MeV and 14.1 MeV neutrons was that one might, to some extent, cancel systematic geometry errors in the calculation of the calibration factors.

As a side effect of making an independent measurement of the 2.5 MeV neutron yield, it was now possible to get a cross calibration with the less sensitive fission chambers. The U-238 fission chamber has not been absolutely calibrated using a neutron source due to its low sensitivity. The calibration was done by the knowledge of the absolute calibration of the more sensitive chambers and a measurement of the relative sensitivities between the chambers. Table 3 shows the neutron counters at ASDEX Upgrade together with the countrate for a linear operating range, the calibration factor and the dead time. The relation between the countrate and the neutron rate is given as:

$$neutronrate = Cal.factor \cdot \frac{Countrate}{1 - Countrate \cdot \tau} \tag{12}$$

where τ is the dead time of the chamber.

Fig. 6 shows the cross calibration between the measurement of the time-integrated yield from In-foils and the U-238 chamber. The measured neutron yield from foil activation is systematically higher than the yield obtained from the fission chamber. It is difficult to know whether the activation method overestimates the yield or if the yield measured by the U-238 chamber is an underestimation. For the activation method, the most uncertain factor is the calculated value of the flux integral (Eq. (10)). The statistical uncertainties are 5-10 % but the systematic error due to the complex modeling for MCNP is difficult to estimate.

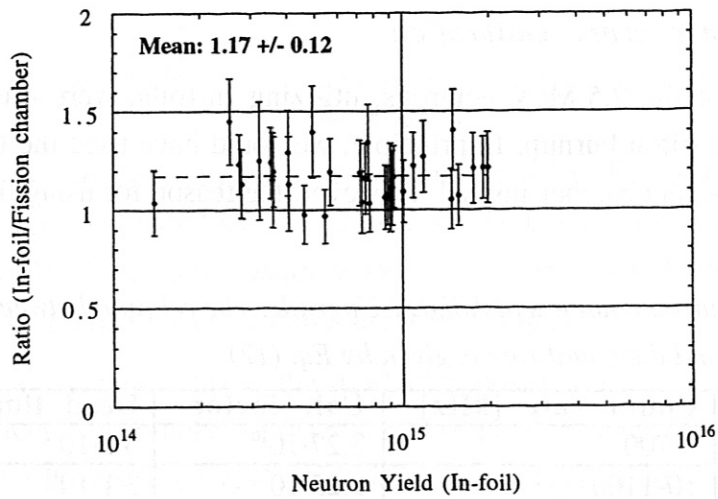

Figure 6. *Cross calibration of the time integrated neutron yields from activation of In-foils and the U-238 fission chamber. Systematically, the yield from neutron activation is 17±12 % higher.*

3.2 Relative calibration of the SBD detector

For a limited period, a silicon surface barrier detector (SBD), located outside the vacuum vessel, was in use [12, 13]. The SBD detector exploits the $^{28}Si(n,p)^{28}Al$ and $^{28}Si(n,\alpha)^{25}Mg$ endoergic reactions in silicon, giving an efficient neutron energy threshold of about 7 MeV. The measurements are time-resolved but routine measurements of the 14 MeV neutrons using SBD are difficult due to the limited lifetime of the diode. The fluency limit at which the diode becomes damaged is about 10^{12} fast neutrons/cm^2. Furthermore is the detector in pulse-counting mode, which means that the dynamic range is limited and the detector becomes easily saturated.

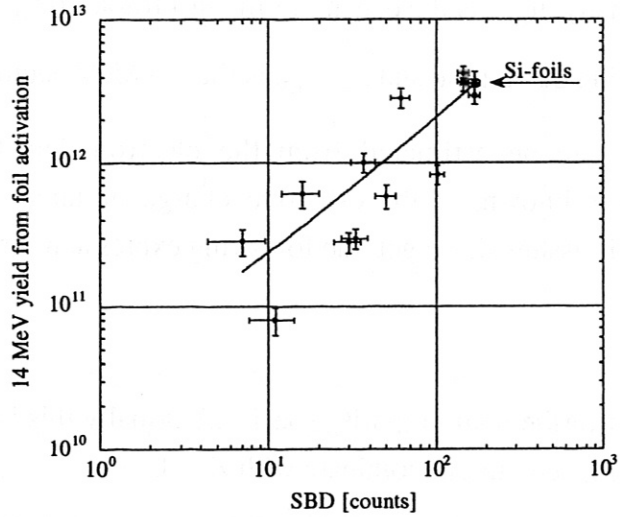

Figure 7. *Neutron yield from activation of copper- and silicon foils versus registered counts from the SBD detector. Two measurements utilizing irradiation of silicon (high performance shots) are included in the plot. The solid line is a simple fit of the data.*

An attempt was made to make a calibration of the SBD detector, utilizing the measured yield by neutron activation of copper and silicon. The result from this measurement is shown in fig. 7. From the figure it is clear that it is difficult to see a clear dependence between the two measurements without more data. However, a simple best linear fit gave $Y_{14.1\,MeV} \approx 2.1 \cdot 10^{10} \cdot Counts_{SBD}$. For the time being, this calibration factor can serve as a rough calibration of the SBD detector.

3.3 Measurements of Triton Burnup

In agreement with other measurements of the triton burnup at different tokamaks [4, 14, 15, 16, 17], the burnup at ASDEX Upgrade lies within an interval of 0.1 - 1.9 % depending on the plasma parameters. The data are scattered and have large errors. The large errors come mainly from the necessity to make two measurements of the irradiated copper foils, which implies a

subtraction of the γ-counts from the measurements. Irradiation of silicon would imply smaller errors of the γ-measurements but then we need higher neutron yields from the plasma. Furthermore, the errors from the copper measurements are not large enough to explain the large deviation of data.

For fully confined tritons, the 14 MeV neutron emission is determined by:

$$\begin{aligned} S_{n:14MeV} &\propto n_D n_{T:fast} \langle \sigma_{DT} v \rangle \\ &\propto n_D \tau_s S_{n:2.5MeV} \langle \sigma_{DT} v \rangle \end{aligned} \tag{13}$$

where n_D is the deuterium density, $n_{T:fast}$ is the density of the fast tritons, $\langle \sigma_{DT} v \rangle$ is the Maxwellian reactivity, τ_s is the triton slowing down time and $S_{n:2.5MeV}$ is the 2.5 MeV neutron emission.

The deuterium density can be estimated from the electron density if the impurity composition of the plasma is known. If the effective charge number, Z_{eff}, is known and quasineutrality of the plasma is assumed, we get the following expression for n_D:

$$n_D = n_e \frac{Z - Z_{eff}}{Z - 1} \tag{14}$$

where Z is the charge number of the main impurity species. Normally this is carbon (i.e. Z = 6). For radiatively cooled plasmas, neon might dominate with Z = 8.

The expression of the triton slowing down time (cf. Eq. (5)) can also be expressed by the "Spitzer slowing down time", $\tau_{Spitzer}$ [18]:

$$\tau_s = \int_{E_0}^{0} \left\langle \frac{dE}{dT} \right\rangle^{-1} dE \propto \tau_{Spitzer} \ln\left(1 + \left(\frac{E_0}{E_{crit}}\right)^{3/2}\right) \propto \frac{T_e^{3/2}}{n_e \ln \Lambda_{ie}} \ln\left(1 + \left(\frac{E_0}{E_{crit}}\right)^{3/2}\right) \tag{15}$$

Now, if Eq. (13) is combined with Eq. (15) we get the following expression for the triton burnup:

$$Burnup \approx \frac{S_{n:14MeV}}{S_{n:2.5MeV}} \propto \frac{Z - Z_{eff}}{Z - 1} \frac{T_e^{3/2}}{\ln \Lambda_{ie}} \ln\left(1 + \left(\frac{E_0}{E_{crit}}\right)^{3/2}\right) \langle \sigma_{DT} v \rangle \tag{16}$$

From Eq. (16) it is realized that the important parameters for fully confined tritons are Z_{eff} and T_e. It should also be emphasized that it is the central plasma parameters, which heavily dominates the triton burnup. The confined fraction is mainly determined by the plasma current which is largest in the plasma center. The deuterium density scales as the electron density (Eq. (14)) which is also highest in the central plasma. Finally, the slowing down time of the tritons, to which the triton burnup is directly proportional (Eq. (13)), scales as $T_e^{3/2}/n_e$ which falls off rapidly with increasing plasma minor radius.

Fig. 8 shows the results from an attempt to show the T_e dependence on the triton burnup (or the triton slowing down time) with Z_{eff} as a parameter. The selected intervals of Z_{eff} were decided by the quality of the best fit to the data. The triton slowing down time was calculated from measured values of n_e and T_e where n_e was measured by DCN-laser interferometer and T_e by Thomson scattering. The values of Z_{eff} were measured by Visible Bremsstrahlung. For the calculation of the deuterium density, n_D, a Z value of 6 was assumed (shots with Ne-puff were excluded from the data analysis).

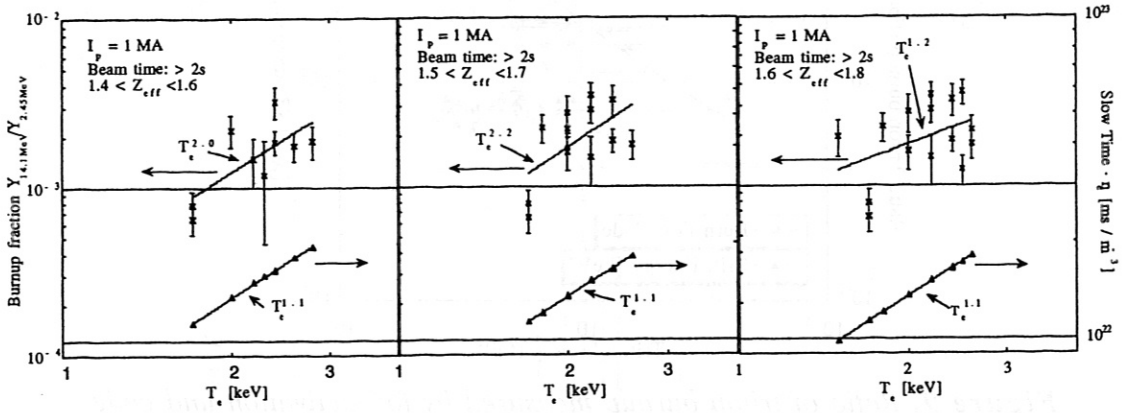

Figure 8. *Measured triton burnup (crosses) and slowing down time multiplied by the electron density (filled triangles) as a function of T_e with Z_{eff} as a parameter. Classically, the triton slowing down time multiplied with the electron density and the burnup should have the same power dependence of T_e. The plasma current is 1 MA for all data. Best fits were obtained when the NBI time was > 2s. The solid lines are power fits of the data.*

It is clear that it is difficult to draw any conclusions from the results shown in fig. 8 except that the triton burnup indeed increases with T_e. First of all, it is necessary to split the data among the values of the Z_{eff}, which leads to very few data remaining for each group. Second, under the assumption that the values of Z_{eff} are reasonable, it is peculiar that the power dependence on T_e varies in such a high degree between the triton burnup and the product of the slowing down time and the electron density. The only T_e power dependence which seems to be reasonable (Burnup~$T_e^{1.2}$), was found for the triton burnup in the $1.6 \leq Z_{eff} \leq 1.8$ range. The reason for the differences in the power dependence of T_e in the $1.4 \leq Z_{eff} \leq 1.7$ range is not clear.

3.4 Calculation of the triton burnup

For the simulation of the burnup fraction, the code CONFINE was used in a time independent version. A full description of the code has been done in ref. [12].

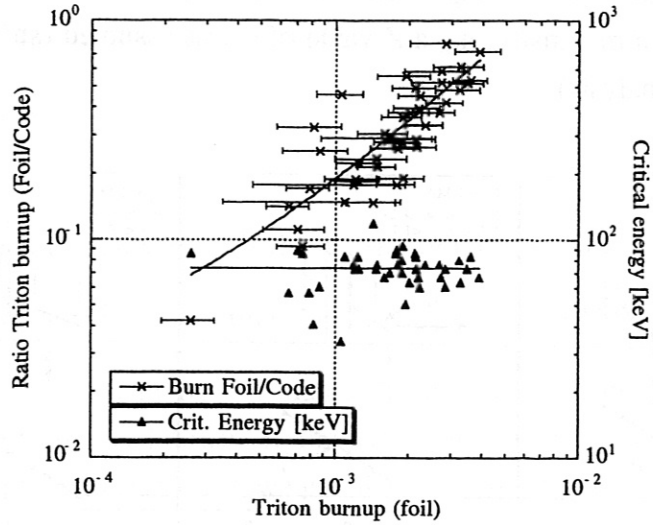

Figure 9. *Ratio of triton burnup measured by foil activation and code calculation. Measured values of the triton burnup are always less than the calculated values but the ratio approaches 1 as the triton burnup increases. The critical energy calculated by Eq. (4) is also indicated. The solid lines are simple fits of the data.*

All calculations are done for circular concentric flux surfaces and only the motion of the gyro center is calculated. Therefore, the shift from the place of birth of the particles to the center of the gyrative motion is neglected. Only at the edge of the plasma, where particles are lost, is the Larmor radius calculated for a check of the prompt losses. Further is it assumed that energy diffusion and pitch angle scattering is negligible and the triton slowing down is assumed to be solely an effect of Coulomb drag on electrons and ions. For the calculation of the probability of burnup it is assumed that the tritons stay on the flux surface where they are born. In reality, they move partly through regions of varying density and temperature, which affects the reaction cross sections. However, this effect can be neglected in most cases [19].

The results from the simulations with the CONFINE code divided with the results from the triton burnup measurements are shown in fig. 9. For all measurements, the measured burnup is less than the simulated one. This was also the case for the triton burnup measurements at TFTR [17].

The reason for the modeled data is consistently larger than the measured data might be explained by the simplifications of the CONFINE code. In ref. [19] the simulated triton burnup for a case was reduced from 1.9 % to 1.1 % by the inclusion of time-dependency, energy diffusion and hot-ion effects. While the time-dependency was responsible for the largest change, the other effects changed the time behavior of the 14 MeV neutron rate significantly. In that paper it was argued that even a small amount of energy diffusion can significantly affect the 14 MeV neutron rate late in time by keeping a larger population of fast tritons around for an extended time period. Therefore the rate increased later in time, by nearly an order of magnitude. However, the net effect was that the inclusion of energy diffusion gave a marginal difference in the burnup.

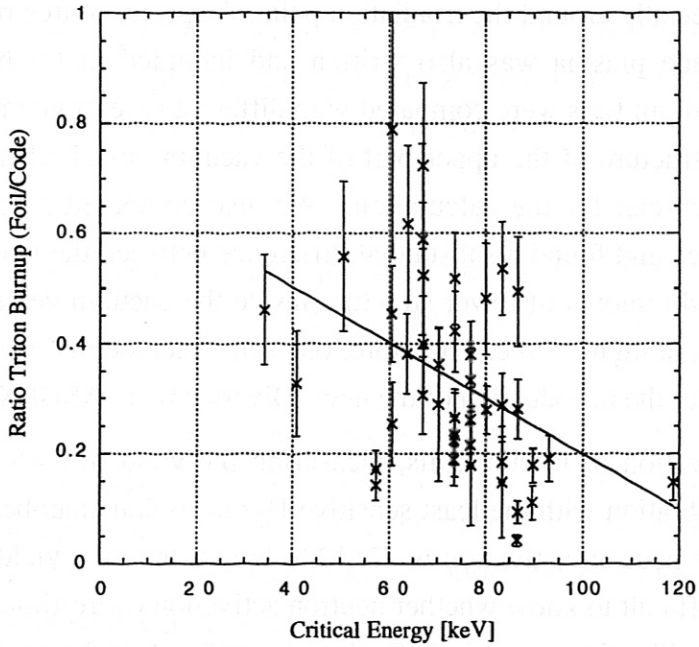

Figure 10. *Ratio of the triton burnup measurement from activation of foils and calculation by the code CONFINE versus the critical energy. There is a tendency that the measured values of the triton burnup becomes "more classical" as the critical energy decreases, i.e. as the ion-drag becomes less important. The solid line is a simple fit to the data.*

In an attempt to find a systematic behavior, the ratio was plotted versus a number of plasma parameters such as, electron temperature, electron density, deuterium density (according to Eq. (14)), effective charge number, Z_{eff}, power and duration of the neutral beam injection and the slowing down time of the tritons. However, no clear trend was seen. The only systematic dependence found, was the ratio versus the measured triton burnup itself. Higher values of the measured triton burnup means that the burnup goes toward the classical regime. When the ratio was plotted versus the critical energy, where the ion-drag equals the electron drag we saw a weak tendency that a small critical energy meant a more classical behavior of the burnup. However,

the effects from both ion-drag and electron-drag are included in the CONFINE code so the reason for the tendency shown in fig. 10 is not clear.

We could not discuss a dependence on plasma current because burnup data are available only for a current of 1 MA and 800 kA. However, no systematic dependence between the ratio and plasma current was found at TFTR either [17].

4 Summary

A system for measurements of the triton burnup using neutron activation of foils, has been installed at ASDEX Upgrade. The calibration factor, relating the global neutron flux to the local flux at the irradiation point, was calculated by MCNP. The input file for MCNP, describing the 3-dimensional geometry of the tokamak, was written with emphasis on the internal structure of the vacuum vessel, especially around the irradiation point. A special source routine, describing a typical ASDEX Upgrade plasma was also written and included in MCNP. The calculated calibration factor for indium foils were compared with different type of geometries (see table 2). It was found that the structure of the upper part of the vacuum vessel, close to the irradiation point, was especially crucial for the calculations. We also compared a line source with our spatially extended source and found a substantial difference between the two cases. A different set of cross sections and removal of lower structure inside the vacuum vessel did not influence the calibration factors in a high degree. Therefore, one can conclude that the calibration factors should be valid even after the introduction of the new "Divertor II" at ASDEX Upgrade.

From neutron activation of indium foils, measuring the yield of 2.45 MeV neutrons, we could make a cross calibration with the least sensitive U-238 fission chamber. It was found that the yield obtained from neutron activation is 17±12 % higher than the yield obtained from the fission chamber. It is difficult to know whether neutron activation overestimates the yield or vice versa. The error of the calibration factor is difficult to quantify while the modeled 3-dimensional geometry is rather complex.

We could also make a rough calibration of a SBD using the results obtained from our 14.1 MeV measurements utilizing copper- and silicon- foils. However, due to the sensitivity of the SBD against radiation damage, the detector was only installed for a shorter period, which meant that the data were few. A rough calibration of the SBD detector gave as result: $Y_{14.1MeV} \approx 2.1 \cdot 10^{10} \cdot Counts_{SBD}$.

The triton burnup was measured by dividing the 14.1 MeV neutron yield obtained from irradiation of copper and silicon foils with the 2.45 MeV yield obtained from indium foils. The results from these measurements gave triton burnup in the interval 0.1-1.9 % depending on the plasma parameters.

The triton burnup and the slowing down time times the electron density, $\tau_s \cdot n_e$, should classically have the same dependency on the electron temperature, T_e. This was indeed the case for the interval $1.6 \leq Z_{eff} \leq 1.8$ where the triton burnup increased as $T_e^{1.2}$. However, for the $1.4 \leq Z_{eff} \leq 1.7$ range the measured burnup showed a much stronger dependency on T_e with a powerfactor of 2.0-2.2. The values of $\tau_s \cdot n_e$ increased as $T_e^{1.1}$ for all values of Z_{eff}. It is clear that we have just a small amount of data available for analysis but unfortunately there has been no clear trend in earlier publications, with more available data, either.

The measured triton burnup was also compared with calculated values, utilizing the code CONFINE. In agreement with earlier comparisons with different codes, the measured triton burnup was always smaller than the calculated values. In earlier works it was suggested that the inclusion of time-dependency in the calculations decreased the calculated burnup. Other effects, e.g. hot-ion effects and energy diffusion, affect the time behavior of the burnup but the integrated burnup is approximately the same as in steady state calculations.

Acknowledgements

One of us (M. Hoek) would like to express his gratitude for the granted EU postdoctoral fellowship that made it possible to work for a period of two years at the ASDEX Upgrade tokamak in Garching bei München.

The first thing that had to be done for the measurements of the triton burnup was to design a rabbit system for the transportation of the foils to a region as close as possible to the plasma. During this design phase we were in constant contact with Hr. Dorn (ASDEX Upgrade) for the design and engineering of the system. Thanks to Hr. Dorns skill and experience, we finally got a system that worked without any problems at all.

For the MCNP calculations of the calibration factor, we are in debt to many people. Especially, we want to express our gratitude to Dr. Fieg and Dr. Fischer from Kernforschungszentrum, Karlsruhe, for the initial modeling of the ASDEX Upgrade tokamak and for the modeling of the plasma source, respectively. By the "inheritance" of the initial modeling of the tokamak, a tremendous amount of time was gained during the MCNP modeling phase. We also want to express our gratitude to the subscribers of the E-mail distribution list of MCNP. When we had questions, we could always count on some very fruitful answers from the subscribers. Especially, we want to thank Dr. Arkuszewski from PSI, Switzerland, for his many prompt answers to our questions.

The knowledge of the Z_{eff} is an important plasma parameter if one want to characterize the behavior of the triton burnup. We are much grateful to Dr. Steuer (ASDEX Upgrade) for the frequent discussions regarding the measurements of, and the calibration procedures for, the values of Z_{eff}.

Finally, warm thanks to Dr. Behler, Dr. Drube and Dr. Merkel for excellent SUN/UNIX support.

References

[1] H.-S. Bosch and G.M. Hale, Nuclear Fusion, 32 (4) (1992) 611

[2] T. H. Stix Plasma Phys. 14 (1972) 367

[3] M. Hoek, T. Nishitani, Y. Ikeda and A. Morioka, Rev. Sci. Instrum. 66 (1) (1995) 885

[4] M. Hoek, T. Nishitani, M. Carlssson and T. Carlsson, Nucl. Inst. Methods, A 368 (1996) 804

[5] E.B. Nieschmidt, T. Saito, C.W. Barnes, H.S. Bosch, and T.J. Murphy, Rev. Sci. Instr., 59 (8) (1988) 1715

[6] MCNP-A General Purpose Monte Carlo Code for Neutron and Photon Transport, LA-7396-M, Rev. 2B, Los Alamos National Laboratory (April 1981)

[7] Report: G. Fieg, "Monte Carlo Calculations with the MCNP Code for Investigations of Neutron and Photon Transport at the ASDEX Upgrade Tokamak". Institut für Neutronenphysik und Reaktortechnik, Projekt Kernfusion. KfK 4851, March 1991.

[8] K.A. Vershuur, "Poloidal Variation of the NET Blanket Nuclear Response Functions", ECN-87-011, Stichting Energieonderzoek Centrum Nederland (1986)

[9] U. Fischer, Fusion Technology, 22 (1992) 251

[10] H. Brysk, Plasma Phys. 15 (1973) 611, and refs. therein.

[11] C.W. Barnes and A.R. Larson, Fusion Technology 30 (1996) 63

[12] Report: W. Ullrich, "Messung sekundärer Fusionsreaktionen in ASDEX Upgrade". Max-Planck-Institut für Plasmaphysik, IPP I/294, Jan. 1996.

[13] W. Ullrich, H.-S. Bosch, F. Hoenen, and ASDEX Upgrade Team, Rev. Sci. Instr., 68 (12) (1987) 4434

[14] J. Källne, G. Gorini, O.N. Jarvis et al., Physica Scripta T16 (1987) 160

[15] J. Källne, P. Batistoni, G. Gorini et al, Nucl. Fusion 28 (7) (1988) 1291

[16] T. Nishitani, M. Hoek, H. Harano, M. Isobe, K. Tobita, Y. Kusama, G.A. Wurden and R.E. Chrien, Plasma Phys. Control. Fusion 38 (1996) 355

[17] C.W. Barnes, H.-S. Bosch et al., Nuclear Fusion 38 (4) (1998) 597

[18] L. Spitzer, "Physics of fully Ionized Gases", Interscience Tracts on Physics and Astronomy, Wiley, New York, 1962.

[19] P. Batistoni and C.W. Barnes, Plasma Physics and Controlled Fusion 33 (14) (1991) 1735